

# Modelling a Linear and Limited Travel Solenoid

N.C. Cheung, K.W. Lim, M.F. Rahman  
University of New South Wales, Australia

**Abstract-** This paper proposes an efficient dynamic model for a solenoid. The magnetic characteristics in the model are based on piecewise approximation with the linear and saturation sections approximated by first order and second order functions respectively. A typical solenoid valve is used to validate the model. Preliminary results show that the model is both accurate and efficient. The model will be used to design a proportional solenoid valve.

## 1. INTRODUCTION

SOLENOIDS are widely used as switching actuators. They are simple in construction, rugged, and relatively cheap to produce. The paper describes part of a project which aims to evaluate the feasibility of using the solenoid as a proportional actuator. This is a non trivial task because of the highly non linear magnetic characteristic of the device.

In this paper we propose a method for dynamic modelling of a linear traverse and limited travel solenoid. Section 2 examines the control dynamics and magnetic characteristics of a solenoid. A method for modelling a solenoid, including its non linear magnetic characteristics, is proposed in section 3. Finally, section 4 validates the model for a typical industrial solenoid by comparing a dynamic simulation of a the device with its experimental measurements.

## 2. CONTROL AND MAGNETIC CHARACTERISTICS OF THE LINEAR TRAVEL VR SOLENOID

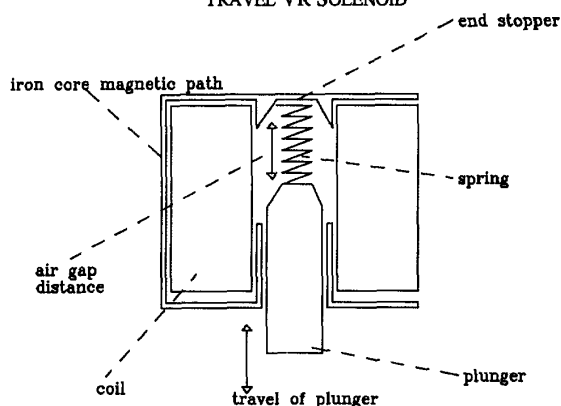


Figure 1. A linear travel VR solenoid

Figure 1 shows the typical construction of a linear and limited travel solenoid. The solenoid's plunger retracts inward when the coil is energised, and extends outward by releasing the stored energy from the spring. Total travel of the plunger is very short: in most cases, it is limited to one centimetre only. In order to achieve a high power to size ratio, most solenoids operate well into the non linear magnetic saturation region.

### 2.1 Dynamic characteristics of a solenoid

A solenoid has a resistive and inductive structure. Its voltage equation can be expressed as:

$$V = Ri + \frac{d\lambda}{dt} \quad (1)$$

where  $V$  is the terminal voltage and  $R$  is the resistance of coil. The flux linkage  $\lambda$ , is a variable dependent on the current of the coil  $i$ , and the air gap distance  $x$ . Therefore the voltage equation can be rewritten as:

$$V = Ri + (L_e + \frac{\partial \lambda(x, i)}{\partial i}) \cdot \frac{di}{dt} + \frac{\partial \lambda(x, i)}{\partial x} \cdot \frac{dx}{dt} \quad (2)$$

$L_e$  is the inductance of the external circuit. There are three terms in the equation (2). The first term is the resistive voltage drop. The second term is the inductive voltage due to change of current. The third term is known as 'back e.m.f.' or 'self e.m.f.' and is caused by the motion of the plunger. Equation (2) can only be solved if the magnetic characteristics of the solenoid are known.

On the mechanical side, the solenoid can be represented by a mass spring system:

$$m_p \ddot{x} = F_{mag} - K_s x - m_p g \quad (3)$$

where  $m_p$  is the mass of the plunger,  $K_s$  is the spring constant,  $g$  is the gravitational constant, and  $F_{mag}$  is the force produced by magnetic field when the coil is energised.  $F_{mag}$  can be calculated from the co-energy  $W'$ . The co-energy can be estimated from the integration of flux linkage against current:

$$F_{mag} = \frac{\partial W'(x, i)}{\partial x} \quad (4)$$

$$W'(x, i) = \int_0^i \lambda(x, i) \cdot di \quad (5)$$

Since the variables  $i$  and  $x$  are fully independent and separable in relation to  $\lambda(x, i)$ , it is permissible to 'differentiate under the integral sign'. Equation 4 and 5 becomes:

$$F_{mag} = \int_0^i \frac{\partial \lambda(x, i)}{\partial x} \Big|_{i=const} \cdot di \quad (6)$$

For instantaneous value of  $F_{mag}$ , when  $x$  does not change during that short period of time, equation (6) can be written as:

$$F_{mag} = \frac{\partial \lambda(x, i)}{\partial x} \cdot i \quad (7)$$

From equations (2), (3), and (7) we can write a non linear state model:

$$\frac{dx}{dt} = v \quad (8)$$

$$\frac{dv}{dt} = \left( \frac{\partial \lambda(x,i)}{\partial x} \cdot i - K_r x - m_p g \right) \cdot \frac{1}{m_p} \quad (9)$$

$$\frac{di}{dt} = \left( V - Ri - \frac{\partial \lambda(x,i)}{\partial x} \cdot \frac{dx}{dt} \right) \cdot \frac{1}{L_r + \frac{\partial \lambda(x,i)}{\partial i}} \quad (10)$$

In equations (8) to (10),  $\partial \lambda / \partial x$  and  $\partial \lambda / \partial i$  are obtained from a model of the magnetic characteristics. A parsimonious model of these characteristics is the key to the usefulness of equations (8) to (10).

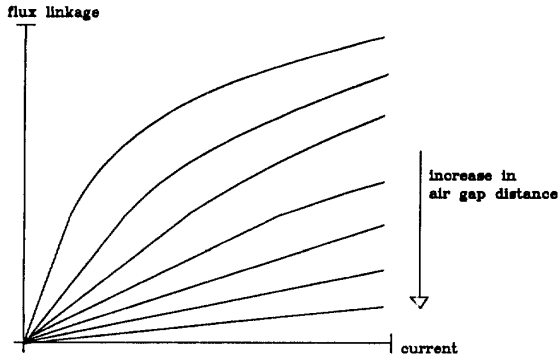


Figure 2. Flux linkage versus current for different plunger pos

### 2.2 Magnetic characteristics of a solenoid

The flux-current-position relation forms a basic characteristic of a solenoid. Since the solenoid operates well into the magnetic saturation region, its characteristics cannot be represented by simple linear equations.

Figure 2 is a typical flux-current plot of a solenoid, with displacement  $x$  as a parameter. The curves show that flux linkage versus current is initially a linear relation. As the flux density increases, the curves become non linear. Also, different air gap positions have different degrees of non linearity.

The magnetic characteristic of a solenoid can also be viewed by plotting flux linkage against air gap position, at various current levels. The resultant plot is shown in figure 3. At high current levels, the curves are packed together. Also, the curves tend to become straight lines as they approach saturation levels.

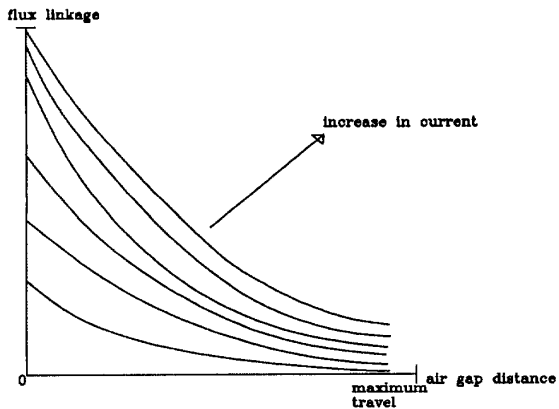


Figure 2. Flux linkage versus plunger position at different current levels

By combining the magnetic characteristics described in section 2.2 with the dynamic equations of (8) - (10), a dynamic model can be obtained.

Several curve fitting techniques are available for describing the magnetic characteristics of a VR machine [1, 2, 3, 4, 5, 6, 7]. However, they are either too complicated to implement in real time [5, 6, 7], or not sufficiently accurate for proportional solenoids [1, 2]. Also, all these methods are designed for use in VR motors only. Solenoids have different magnetic characteristics.

This paper uses a curve fitting technique adapted from [4], but modified for use in linear travel proportional solenoids. The magnetic characteristic is divided into linear and saturated regions. A simple relation based on linear magnetic principles is used for the linear model. This is described in section 3.1. For the saturated region, a parabolic curve approximation is used for the flux linkage versus current curves; and a  $1/x$  function approximation is used for the flux linkage versus position curves. Section 3.2 describes this. The proposed model provides a good balance between accuracy and computational efficiency.

### 3.1 The linear region

Description of the linear region can be obtained by using standard electromagnetic principles based on linear magnetic circuit [10]. Consider a solenoid which operates within its linear region, and has the following parameters:

- Equivalent cross sectional area for iron core and air gap:  $A$
- Effective core length:  $l$  Air gap length:  $x$
- No. of turns of coil:  $N$  Current through coil:  $i$
- Permeability of free space:  $\mu_0$  Relative permeability:  $\mu_r$
- Magnetic flux:  $\Phi$

$$Ni = \frac{l\Phi}{\mu_0 \mu_r A} + \frac{x\Phi}{\mu_0 A} \quad (11)$$

The solenoid can be viewed as a variable structure magnetic circuit, with a m.m.f. equation as in equation (11). It contains two terms; the first term describes the m.m.f. drop due to the iron core, and the second term is the m.m.f. drop due to the air gap.  $\mu_r$  is treated as constant, since it operates below the saturation region. By substituting  $\lambda = N\Phi$ , equation (10) can be rearranged as:

$$\lambda(x,i) = \frac{\mu_0 AN^2 i}{\frac{l}{\mu_r} + x} \quad (12)$$

By introducing two constant terms,  $K_a$  and  $K_b$ , equation (12) can be simplified as:

$$\lambda(x,i) = \frac{K_a}{K_b + x} \cdot i \quad (13)$$

$K_b$  is an approximate constant, in spite of the fact that it changes with the plunger position. This is because  $K_b$  is much smaller than  $x$  for most of the time, and has little effect on the overall equation, except when  $x$  is close to zero. When  $x$  is very close to zero, the percentage of variation of  $K_b$  is very small and can be neglected.

Since flux leakage exists in solenoid, and a proportional amount of current is being used up as leakage flux. Due to this, equation (13) has to be compensated by offset1 as shown in equation (14):

$$\lambda(x,i) = \left( \frac{K_a}{K_b + x} - offset1 \right) \cdot i \quad (14)$$

$K_a$ ,  $K_b$ , and  $offset1$  determines the linear portion of magnetic characteristics; these parameters are obtained by curve fitting equation (14) to the measured values of flux linkage versus position at  $i=i_s$ , by using a standard mathematical software package.

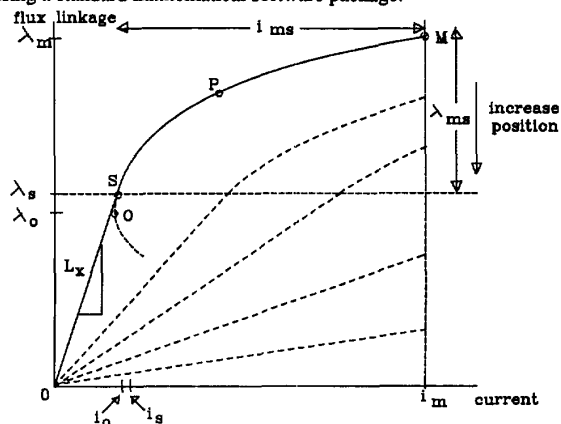


Figure 4. Curve fitting the magnetic characteristic of a VR solenoid by linear and parabolic approximation

### 3.2 Flux linkage versus current

Equation (14) is the general equation for describing the magnetic behaviour of a VR solenoid in the linear region. For the non linear region, the non linear plots are approximated by parabolic curves as shown in figure 4. The parabolic curve has a curvature of  $K_p$  with an origin point of  $O(i_0, \lambda_0)$ . It is represented by equation (15).

$$(\lambda_p - \lambda_0)^2 = 4K_p(i_p - i_0) \quad (15)$$

In figure 4,  $\lambda_s$  is the flux saturation boundary, above which saturation will occur,  $P(i_p, \lambda_p)$  is a point along the flux-current curve with position equal to  $x$ .  $L_x$  is the gradient of the linear part of the flux-current plot, and is obtained by:

$$L_x = \frac{\lambda}{i} = \frac{K_a}{K_b + x} - offset1 \quad (16)$$

The saturation current  $i_s$ , can be obtained from the gradient  $L_x$  by:

$$i_s = \frac{\lambda_s}{L_x} \quad (17)$$

In order to have a smooth transition between the linear and the non linear region, the gradient of the parabolic curve at point  $S(i_s, \lambda_s)$  must be equal to the gradient in the linear region. Using this rule,  $i_0$  and  $\lambda_0$  can be found:

$$i_0 = i_s - \frac{K_p}{L_x^2} \quad (18)$$

$$\lambda_0 = \lambda_s - \frac{2K_p}{L_x} \quad (19)$$

The curvature of the curve is set so that the locus of the parabola will intersect point  $M(i_m, \lambda_m)$ :

$$K_p = \frac{\lambda_{ms}^2}{4(i_{ms} - \frac{\lambda_{ms}}{\lambda_m})} \quad (20)$$

$$\text{where } \lambda_{ms} = \lambda_m - \lambda_s \quad i_{ms} = i_m - i_s$$

This method constructs a parabolic curve based on two coordinates,  $M(i_m, \lambda_m)$  and  $S(i_s, \lambda_s)$  only. Since  $\lambda_s$  and  $i_m$  are predetermined values, therefore only  $i_s$  and  $\lambda_m$  needs to be determined.  $i_s$  can be obtained from equation (15). whereas  $\lambda_m$  can be obtained from a simple look up table of flux against position at  $i_m$ . Alternatively,  $\lambda_m$  can be calculated from the following equation:

$$\lambda_m = \frac{K_c}{K_d} - offset2 \quad (21)$$

$K_c$ ,  $K_d$ , and  $offset2$  are found by curve fitting equation (21) to the flux linkage against position curve when  $i=i_m$ .

With this approach, flux linkage against current relation can be calculated by the following parameters with equations (16)-(21):  $K_a$ ,  $K_b$ ,  $K_c$ ,  $K_d$ ,  $\lambda_s$ ,  $i_m$ ,  $offset1$ , and  $offset2$ .

### 3.3 Flux linkage versus position

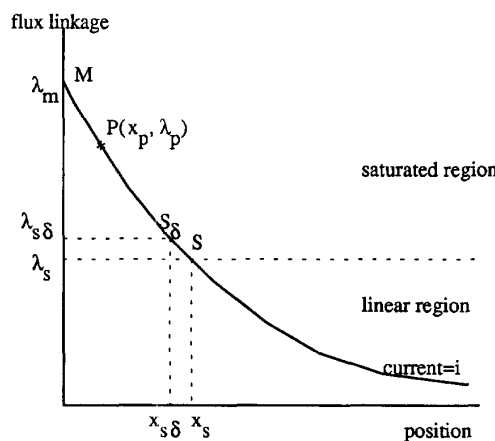


Figure 5. Modelling the saturation region by  $1/x$  approximation

Figure 5 is a typical curve of flux linkage against position for a solenoid. The curve in the linear region can be represented by equation (13). For the saturated region, the curve can be approximated by a  $1/x$  function. The function has the following form:

$$\lambda_p = \frac{K_1}{K_2 + x_p} - K_3 \quad (22)$$

To have the above function pass through point  $M(0, \lambda_m)$ ,  $K_1$ ,  $K_2$ , and  $K_3$  are specified as follows:

$$K_1 = K \cdot S_c \cdot \lambda_m \quad K_2 = K \quad K_3 = (S_c - 1) \cdot \lambda_m \quad (23)$$

The value of  $K$  and  $S_c$  are selected so that the curve of described by equation (22) passes through point  $S$  and  $S_\delta$ . By using the equation in the linear region,  $x_s$  can be obtained:

$$x_s = \frac{K_a}{offset1 + \frac{\lambda_s}{i}} - K_b \quad (24)$$

Point  $S_8(x_{s8}, \lambda_{s8})$  lies to the left and very close to point  $S(x_s, \lambda_s)$ . It is defined by the following relations:

$$x_{s8} = x_s - \delta \quad (25)$$

$$\lambda_{s8} = \left( \frac{K_a}{K_s + x_{s8}} - \text{offset1} \right) \cdot i \quad (26)$$

By referring to equations (22) and (23), the following equations can be formed:

$$\lambda_s = \frac{K \cdot S_c \cdot \lambda_m}{K + x_s} - (S_c - 1) \lambda_m \quad (27)$$

$$\lambda_{s8} = \frac{K \cdot S_c \cdot \lambda_m}{K + x_{s8}} - (S_c - 1) \lambda_m \quad (28)$$

Once  $\lambda_m$  is obtained, the above two equations are used to solve  $K$  and  $S_c$ .  $K$  and  $S_c$  can be calculated as follows:

$$S_c = \frac{ac - c}{\frac{ac}{a} - 1} \quad K = x_s \cdot \frac{S - b}{b} \quad (29)$$

where  $a = \frac{x_s}{x_{s8}}$        $b = 1 - \frac{\lambda_s}{\lambda_m}$        $c = 1 - \frac{\lambda_{s8}}{\lambda_m}$

This method constructs a  $1/x$  function curve based on points  $M$ ,  $S$  and  $S_8$  only.  $\lambda_m$  can be obtained from a table of flux linkage against current when position  $x=0$ . Alternatively,  $\lambda_m$  can be calculated from the parabolic curve as described in the previous section. In this case,  $K_p$ ,  $\lambda_0$ , and  $i_0$  at  $x=0$  should be predetermined to enable faster calculation. With this approach, flux linkage versus position can be calculated by  $K_a$ ,  $K_b$ , offset1, and  $\lambda_s$  by using equations (22)-(26) and (29).

#### 4. EXPERIMENTAL DETERMINATION OF MAGNETIC CHARACTERISTICS

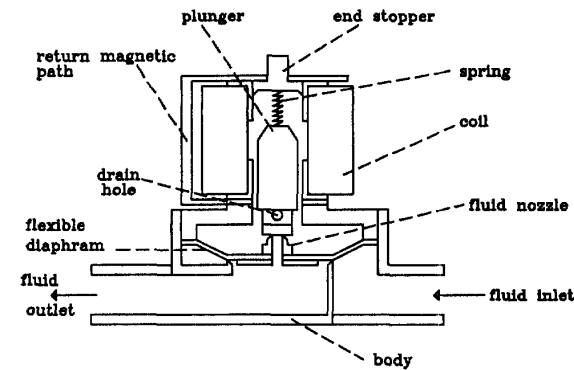


Figure 6. A two stage solenoid valve

This section will describe the experimental procedures for magnetic characteristic determination, dynamic modelling, and dynamic simulation of a typical industrial linear travel solenoid valve. The valve is a two stage 24V d.c. valve that accepts a maximum continuous current of 0.6A. The two stage solenoid valve is shown in figure 6. For the initial study on the solenoid valve, only the plunger, coil and magnetic circuit is of interest.

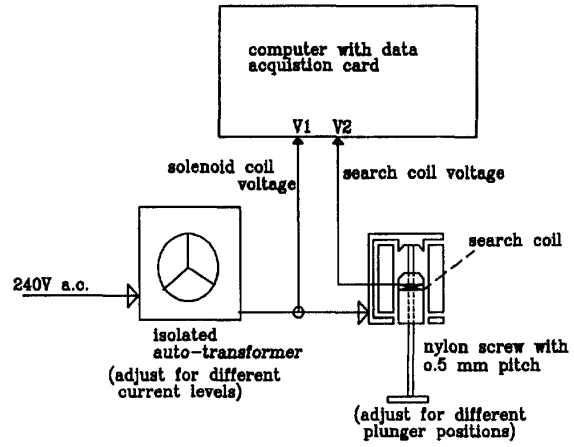


Figure 7. Experimental set up for the determination of magnetic characteristic of the solenoid

#### 4.1 Magnetic characteristic determination

There are two basic ways of obtaining the flux linkage data from a VR machine. The first method is to feed a predetermined d.c. current into the coil, and move the plunger to obtain a variation of flux [8]. The second method is to input a sinusoidal voltage waveform into the coil, and measure the flux change at different locations [8,9]. Unlike the rotary motor, it is very difficult to oscillate the plunger accurately, hence the second method is more appropriate for a linear travel solenoid.

The experimental setup is shown in figure 7. An a.c. voltage is applied to the solenoid coil when the induced e.m.f. from the search coil is measured at different coil currents and plunger positions [11].

Flux linkage  $\lambda(t)$  can be obtained by:

$$\lambda(t) = \left( -\frac{1}{N_s} \int e(t) \cdot dt \right) \cdot N \quad (30)$$

where  $N$  is the number of turns of solenoid's coil,  $N_s$  is the number of turns of search coil, and  $e(t)$  is the induced e.m.f.

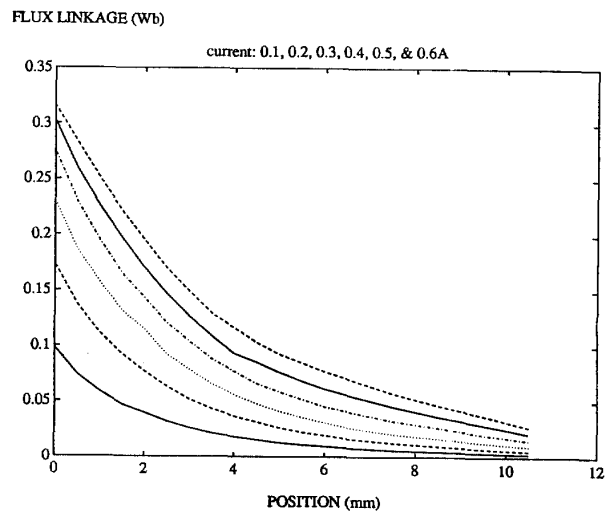


Figure 8. Flux linkage vs. position measurements from a solenoid

Using the above equation, a series of hysteresis shaped curves for each plunger position are produced. By joining the vertex of the hysteresis shaped curves, plots for flux linkage against position (figure 8) and flux linkage against current (figure 9) are produced.

The a.c. excitation search coil method produces very accurate result, since the plunger is stationary during measurement. Also, it eliminates synchronisation and transient switching problems found in methods based on step voltage energisation and current rise/decay measurement [9].

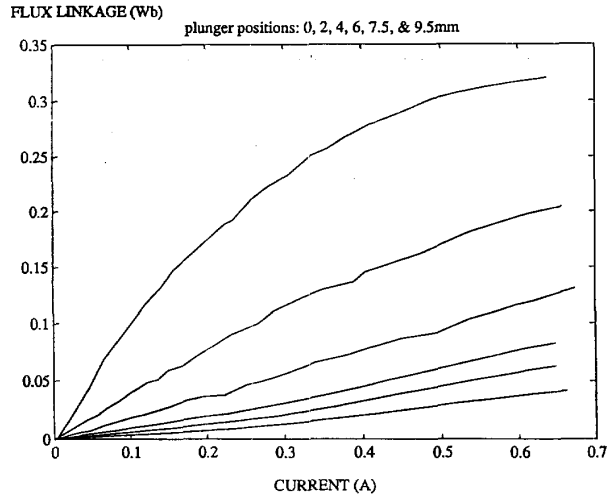


Figure 9. Measurement of flux linkage versus current of a solenoid.

#### 4.2 Magnetic characteristics approximation

To obtain the required parameters for the magnetic characteristics approximation,  $K_a$ ,  $K_b$ ,  $K_c$ ,  $K_d$ , offset1, and offset2, are obtained by curve fitting equations (14) and (21) to the measured data shown in figure 8.  $\lambda_c$  is found from the graph of figure 9. Figure 10 and 11 are the magnetic model of flux linkage against current, and flux linkage against position respectively. When compared to the actual measured data, they are very similar.

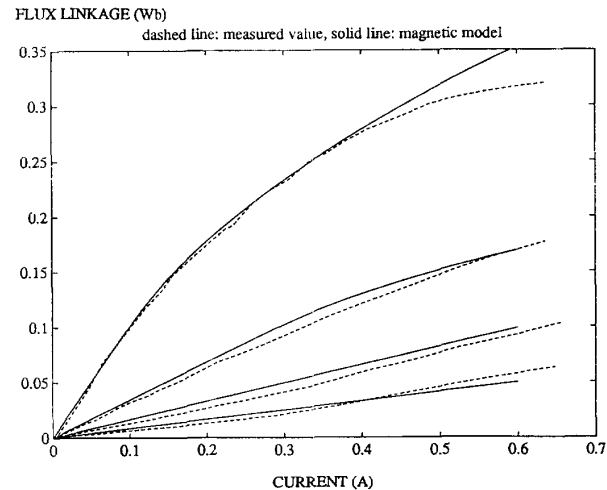


Figure 10. Comparison of the magnetic model with the actual measured values. (flux linkage vs. current)  $x=0, 2.5, 5, \& 7.5\text{mm}$

For the model of flux linkage against current, the curve fitting error is less than  $\pm 0.02\text{Wb}$  over range of 0 to  $0.3\text{Wb}$ . For the very small operational area above  $0.3\text{Wb}$ , this error jumps up to  $+0.04\text{Wb}$ . The curve fitting error over the whole operating range of 0 to  $0.35\text{Wb}$  for the flux linkage versus position plot is less than  $\pm 0.02\text{Wb}$ . However, the error gets progressively worse when it goes over its operation point. Overall, this magnetic model is much more accurate than piecewise linear approximations [1,2]. It provides a smooth transition between the linear and saturated sections.

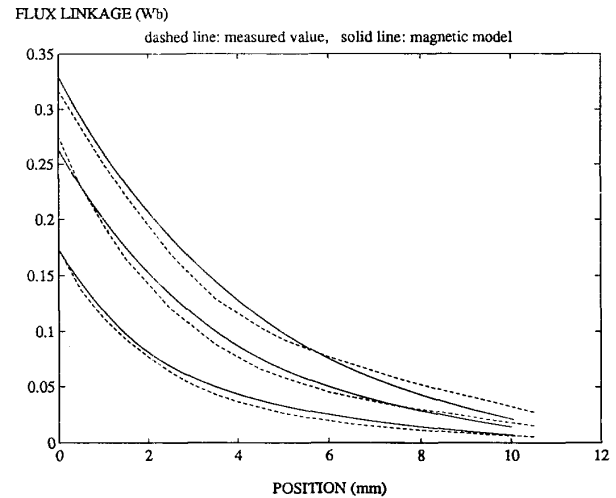


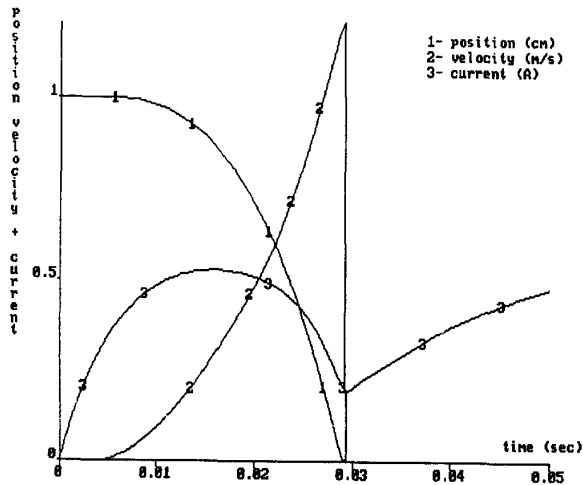
Figure 11. Comparison of the magnetic model with the actual measured values. (flux linkage versus position).  $i=0.2, 0.4, \& 0.6\text{A}$

#### 4.3 Validating the dynamic model of the solenoid valve

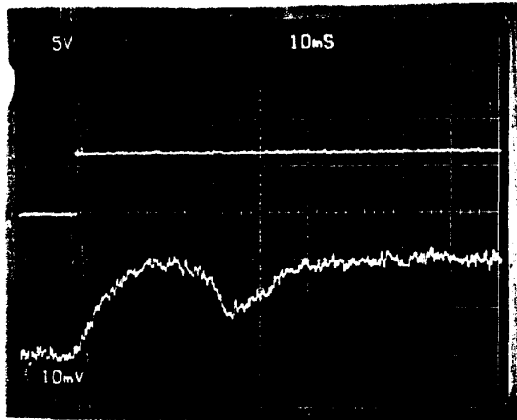
By combining the magnetic model with equations (8)-(10), a dynamic model is formed. The accuracy of the dynamic model is validated by simulating its transient response. Figure 12 compares a simulation of the solenoid's dynamic model with experimental results. The step response is reasonably accurate. Detail validation results will be presented at the conference. Figure 13 is a comparison of the simulation result with the actual measured result under extreme condition when the magnetic approximation is least accurate. Under this operating region, the simulation result is very sensitive to parameter variation, especially on the prediction of force.

## 5. CONCLUSION

This paper proposes a computationally efficient dynamic model for a proportional solenoid. The model is being applied to a commercial solenoid with a curve fitting error of less than  $\pm 0.02\text{Wb}$  out of the operating range of  $0-0.32\text{Wb}$  for 98% of its operating area. The complete dynamic model is verified experimentally. Under normal operating condition, its simulated transient response is very similar to the actual measured transient response of the solenoid.

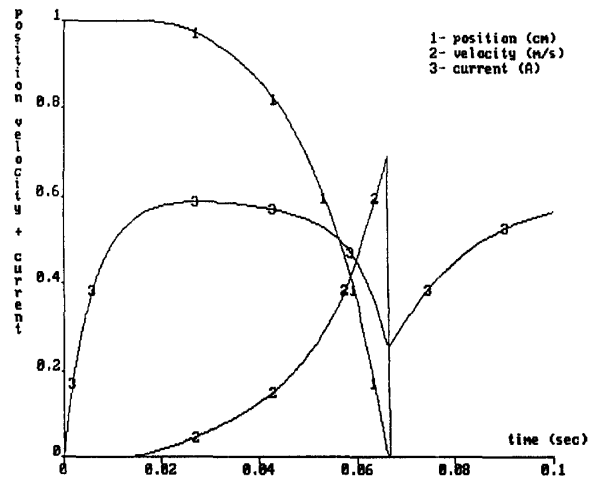


(a)

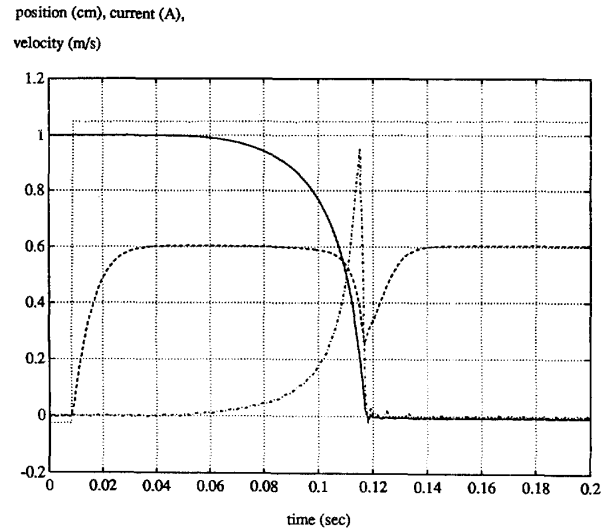


(b)

Figure 12. Simulation result (a) and actual measurement (b) of a solenoid's dynamic response.



(a)



6. REFERENCES

- [1] H.D. Chai, "A mathematical model for single stack step motors", IEEE Trans Power Apparatus and Systems, PAS-94, pp1508-1517, 1975.
- [2] R. Krishnan, R. Arumugam, and J.F. Lindsay, "Design procedure for switched reluctance motors," IEEE Trans. on Industry Applications, vol. 24, no. 3, pp 456-461, May/June 1988.
- [3] S. Bolognani, G.S. Buja, and M.I. Valla, "Switched reluctance motor performance analysis based on an improved modelling of its magnetic characteristics," Electric Machines and Power Systems, vol. 19, iss. 4, pp 425-438, Jul/Aug 1991.
- [4] T.J.E. Miller and M. McGilp, "Non linear theory of the switched reluctance motor for rapid computer aided design," IEE Proc. vol 137, pt. B, no. 6, pp 337-346, Nov 1990.
- [5] D.A. Torrey and J.H. Lang, "Modelling a non linear variable reluctance motor drive," IEE Proc. vol. 137, pt. B, no. 5, pp 314-326, Sept 1990.
- [6] D.G. Manzer, M. Varghese, and J.S. Throp, "Variable reluctance motor characterization," IEEE Trans. on Industrial Electronics, vol. 36, no. 1, pp 56-63, Feb 1989.
- [7] J.M. Stephenson and J. Corda, "Computation of torque and current in doubly salient reluctance motors from non linear magnetisation data", IEE Proc., pt. B, vol. 126, pp 393-396, 1979.
- [8] A. Ferro and A. Raciti, "A digital method for the determination of magnetic characteristics of variable reluctance motors," IEEE Trans. on Instrumentation and Measurement, vol 39, no. 4, pp 604-608, Aug 1990.
- [9] R. Krishnan and P. Materu "Measurement and instrumentation of a switched reluctance motor," IEEE Industry Applications Society annual meeting, 1989, vol 1, pp 116-121.
- [10] A.E. Fitzgerald, "Electric Machinery: the processes, devices, and systems of electro-mechanical energy conversion," McGraw Hill, 1971.
- [11] N.C. Cheung, M.F. Rahman, K.W. Lim, "Simulation and experimental studies towards the development of a proportional solenoid," Australian Universities Power Engineering Conference, Sept 1993.